International Journal of Chemical, Materials and Biomolecular Sciences
ISSN: 2415-6620
Vol:8, No:10, 2014

The Effect of Porous Alkali Activated Material Composition on Buffer Capacity in Bioreactors

G. Bumanis, D. Bajare

***Abstract*—**With demand for primary energy continuously growing, search for renewable and efficient energy sources has been high on agenda of our society. One of the most promising energy sources is biogas technology. Residues coming from dairy industry and milk processing could be used in biogas production; however, low efficiency and high cost impede wide application of such technology. One of the main problems is management and conversion of organic residues through the anaerobic digestion process which is characterized by acidic environment due to the low whey pH (<6) whereas additional pH control system is required. Low buffering capacity of whey is responsible for the rapid acidification in biological treatments; therefore alkali activated material is a promising solution of this problem. Alkali activated material is formed using SiO_2 and Al_2O_3 rich materials under highly alkaline solution. After material structure forming process is completed, free alkalis remain in the structure of materials which are available for leaching and could provide buffer capacity potential. In this research porous alkali activated material was investigated. Highly porous material structure ensures gradual leaching of alkalis during time which is important in biogas digestion process. Research of mixture composition and SiO_2/Na_2O and SiO_2/Al_2O ratio was studied to test the buffer capacity potential of alkali activated material. This research has proved that by changing molar ratio of components it is possible to obtain a material with different buffer capacity, and this novel material was seen to have considerable potential for using it in processes where buffer capacity and pH control is vitally important.

***Keywords*—**Alkaline material, buffer capacity, biogas production.

I. Introduction

BIOGAS technology provides an alternative source of energy to fossil fuels in many parts of the world. Using local resources such as agricultural crop remains, municipal solid wastes, market wastes and animal waste, biomass and manure are derived by anaerobic digestion. The hydrolysis process, where the complex insoluble organic materials are hydrolysed by extracellular enzymes, is a rate-limiting step for anaerobic digestion of high-solid organic wastes.

To ensure maximum yield of methane gas, environment with optimum conditions for microorganisms must be provided in the biogas reactors. Anaerobic treatment of substrates has therefore frequently encountered difficulties in maintaining stable operation [1], [2]. It is characterised by a very high organic load and low buffer capacity; consequently, the direct anaerobic treatment of substrate can lead to rapid acidification which results in low biogas productivity [3]. As most of the substrates have low bicarbonate alkalinity and tend to acidify rapidly, supplemental alkalinity is required so as to avoid anaerobic process failure. Most microorganisms grow within a fairly narrow pH range, therefore pH adjustment is necessary to increase the yield of methane [1]. Novel material described in this paper belongs to the group of alkali activated materials (AAM) and deals with the complex solution for biogas technology; simultaneously it obtains properties appropriate for immobilisation of microorganisms in anaerobic reactors and pH adjustment over some time.

The initial results showed that the alkaline materials, which have been introduced in the biogas digestion processes, increased methane potential up to 1.9–2.5 times compared to the manual pH controlled digestion process [4].

AAM are made by mixing solid aluminosilicate powders such as fly ash, blast furnace slag, or metakaolin with an alkaline activating solution. The reaction product or gel have a network structure similar to those of organic thermoset polymers, and thus the binders are sometimes called “inorganic polymers” or “geopolymers” [5]. The detailed chemistry of alkali activation is still the subject of much discussion in the scientific literature and depends on the nature of both the solid precursor and the alkali activator selected – namely, on aluminosilicate systems activated with alkali metal hydroxide, silicate or solutions from both of them.

Traditionally nature of the binder gel is determined mainly by the level of calcium available for the reaction. For example, a high-calcium alkali-activated binder (made of blast furnace slag) usually forms a primary binder phase of C–(A)–S–H gel that is amorphous to partially crystalline, relatively highly cross-linked, with a moderate degree of Al substitution and a low C/S ratio [6], [7]. Whereas lower levels of calcium in solid precursor lead to the presence of what is widely referred to as a “geopolymer” gel, which is a highly cross-linked aluminosilicate gel bearing strong nanostructural rebalance to zeolite frameworks but is generally lacking in long-range crystalline order [5], [8], [9].

Many authors have found that the product of activated metakaolin (activated with NaOH solutions) is N–A–S–H gel with good durability and mechanical properties [10]-[12]. The general formula for the reaction product is $2SiO_2 \cdot Al_2O_3 \cdot Na_2O \cdot 2H_2O$ [6]. When the activator is a NaOH and waterglass mix, the material formed also is amorphous and cementitious, but its structure and composition are different from the product formed when NaOH alone is used: the amorphous N–A–S–H gel has thus similar chemical

G. Bumanis is with the Institute of Materials and Structures, Riga Technical University, Kalku str.1, Riga, LV-1016, Latvia. (phone: 371-26062011; fax: 371-67089142; e-mail: girts.bumanis@rtu.lv).

D. Bajare, is with the Institute of Materials and Structures, Riga Technical University, Kalku str.1, Riga, LV-1016, Latvia. (phone: 371-29687085; e-mail: diana.bajare@rtu.lv).

composition as natural zeolite materials but without the extensive crystalline zeolite structure [13],[14].

It has been reported that the formation of geopolymer gel is greatly dependent on the pH of activator and Si/Al ratio of solid precursor [15]-[18].

Analysis showed that dissolution of metakaolin and formation of new minerals occurred faster in the hydroxide-activated geopolymer system, probably due to the high pH. The silicate activating solution is of lower pH, leading to a slower rate of reaction, and shows a strong signal attributed to unreacted aluminium in metakaolin particles early in the reaction process [9].

The complicating factor in the geopolymerization process is the general decrease in aluminium content of the materials with high calcium content. It would be expected that tetrahedral aluminium would remove alkali cations from the pore solution and incorporate them into the gel, as has been previously observed for metakaolin-derived alkali aluminosilicate (geopolymer) gels and for calcium aluminosilicate hydrate (C–A–S–H) gels [19]-[21]. Consequently, a decrease in the aluminium content of the binder would be expected to increase the amount of alkali remaining in the pore solution [22]. However, none of the studies showed a particularly strong correlation between dissolved Al and Na concentrations. Similar, the alkali content in the pore solution increase with the increase of alkali content in the activating solution. The increase is approximately proportional, with the exception of samples with very low alkali content (3wt.% Na_2O) [22].

The composition of the binder clearly has an important effect on the diffusion of alkali from geopolymers; in particular, the absence of calcium was important for increasing alkali mobility. Geopolymers containing significantly lower levels of calcium (*i.e.* metakaolin) appear to have approximately 10-fold higher effective diffusion coefficients than their high-Ca counterparts. It is apparent that the pore solution of thermally cured low-calcium geopolymers contains a high concentration of alkali metal cations; typically more than 500mM and in several cases greater than 1M [22]. Given the low concentration of aluminate and silicate counter-ions, it may be concluded that neutrality is maintained primarily by hydroxyl ions. This would provide the pore solution with a high pH and would be expected to be used for pH adjustment in the biogas reactors.

Effect of mixture composition of the AAM was studied in this research. By changing Al_2O_3, SiO_2 and Na_2O source, AAM with different SiO_2/Al_2O_3 and SiO_2/Na_2O ratios can be created. Buffer capacity as $CaCO_3$ equivalent, namely, in mg per L solution per g of material ($CaCO_3$eq mg/l/g) was studied.

II. Materials and Methods

A. Materials

Alkali activating technology provides the possibility to use wide group of alumina and silica rich materials as raw materials to create AAM. This technology allows reutilizing production waste materials, which makes the technology environmentally friendly. Secondary raw materials were used to create AAM in this research: waste metakaolin (MK), nonmetallic residues (NMR) from the aluminium scrap recycling factory and lead-silica glass (LSG) from fluorescent lamp recycling process.

MK was obtained from expanded glass granule production plant in Lithuania, where kaolinite clay is used as a substance for anti-agglutination in the final stage of expanded glass granule production. During production MK was calcined at 850°C for about 40-50minutes and fraction <0.25mm was sieved as MK powder.

NMR from the aluminium scrap recycling factory was used as Al_2O_3source and pore creating agent. The exact chemical and mineralogical composition as well as other properties of NMR are provided in the previously published papers [23], [24].

The lead-silica glass (LSG) was obtained from fluorescent lamp recycling process, which includes lamp classification, glass separation, cleaning from harmful components and glass grinding.

In order to increase homogeneity and fineness of NMR and LSG, both materials were ground for 30 minutes by using planetary ball mill Retsch PM 400. The chemical composition of MK, NMR and LSG is given in Table I.

TABLE I
Chemical Composition of Raw Materials, w_t%

Chemical component	NMR	MK	LSG
Al_2O_3	63.19	51.7	1.03
SiO_2	7.92	34.4	68.07
CaO	2.57	0.09	1.39
SO_3	0.36	-	-
TiO_2	0.53	0.55	-
MgO	4.43	0.13	-
Fe_2O_3	4.54	0.53	0.19
PbO	-		20.02
Na_2O	3.84	0.63	8.02
K_2O	3.81	0.01	1.17
Other	2.6	-	0.11
LOI, 1000°C	6.21	12.1	-

The AAM were prepared by using alkali activator solution (AAS) with silica modulus Ms 1.67. Alkali activators were prepared by using commercially available sodium silicate solution characterized by the silica modulus Ms3.22. To obtain alkali activation solution with the required chemical composition, the modification with an addition of sodium hydroxide was done. Commercially available sodium hydroxide flakes with 97% purity were used.

B. Methods

Physical properties of AAM, such as density, water absorbtion, open and total porosity, were determined in accordance with EN 1097-6 and EN 1097-7.

Alkalinity is defined as a measure of the buffering capacity of water to neutralize acid. This capacity is attributed to bases that are present in natural waters including OH^-, HCO_3^-, and

CO_3^{2-}. High alkalinity in water indicates increased buffering capacity.

The buffer capacity was tested for 3 days old AAM by immersing cubical specimens (weight 3.5±0.5g) in the deionized water and measuring the alkalinity dynamics within 30 days. Samples were moved to a new bath with deionized water (100 ml) with interval 24h. pH of water solution was determined and alkalinity in mg/l/gas $CaCO_3$ equivalent per 1g of AAM was calculated.

In order to determine alkalinity, samples were titrated with hydrochloric acid 0.01M to a certain pH end point (pH 8.3 for CA and pH 4.5 for BCA and TA). Total (TA), carbonate (CA) and bicarbonate (BCA) alkalinities in deionized water from all samples were measured every day.

The following reactions were occurring during titration[25]: pH range: above 8.3

$$OH^- + H^+ \rightarrow H_2O \quad (1)$$

$$CO_3^{2-} + H^+ \rightarrow HCO_3^- \quad (2)$$

pH range: between 8.3 and 4.5

$$HCO_3^- + H^+ \rightarrow H_2CO_3 \quad (3)$$

Equation (1) was used to calculate TA, (2) for BA and (3) for BCA respectively[25]:

$$TA = V_{t1} \cdot M \cdot C \cdot V^{-1} \cdot m^{-1} (mg \cdot l^{-1} \cdot m^{-1}) \quad (4)$$

$$CA = V_{t2} \cdot M \cdot C \cdot V^{-1} \cdot m^{-1} (mg \cdot l^{-1} \cdot m^{-1}) \quad (5)$$

$$BCA = V_{t3} \cdot M \cdot C \cdot V^{-1} \cdot m^{-1} (mg \cdot l^{-1} \cdot m^{-1}) \quad (6)$$

where

V_{t1} – volume of standard acid solution (ml) to pH 4.5;

V_{t2} – volume of standard acid solution (ml) to pH 8.3

V_{t3} – volume of standard acid solution (ml) from pH 8.3 to pH 4.5

M –concentration of acid (mol l^{-1});

C – 50 000 (mg $CaCO_3$/eq).

V – volume of sample, ml;

m – mass of AAM sample, g.;

Scanning electron microscope (SEM) (Tescan Mira/LMU) was used for microstructural characterization of AAM. BET method (QuadraSorb) was used to determine surface area of AAM.

III. Mixture Composition and Sample Preparation

Three mixture compositions with different proportion of the solid raw materials s were chosen. First composition (S0) consisted of NMR, MK and LSG with ratio 1:1:0, second – with ratio 1:1:1 (S1) and third –with ratio 2:1:1 (Al2S1) respectively. NMR is a pore structure forming substance, therefore mixture composition Al2S1 was prepared for amount of the pore forming agent to remain constant comparing to mixture S0. For each of these three mixture compositions four different alkali activator solution/solid ratios (AAS-solid ratio) were chosen – 0.30, 0.45; 0.60 and 0.75. SiO_2/Al_2O_3 and SiO_2/Na_2O ratios of all compositions were calculated (Table II). SiO_2/Al_2O_3 was in range from 0.77-1.91, SiO_2/Na_2O from 3.23-5.08 and Na_2O/Al_2O from 0.17-0.52. Incorporation of LSG and increase of AAS-solid ratio in mixture composition increased amount of $SiO_2$and Na_2O in AAM composition; therefore total increase of leaching alkalis has been expected (for mixtures Al2S1 and S1).

The solid raw materials were mixed together and AAS were added. To ensure workability for mixtures with lower AAS-solid ratio, additional water was added. After mixing, the pastes were immediately poured into sealed prismatic moulds measuring 4×4×16 cm. The amount of paste poured into the mould was calculated according to the expansion of each mixture for avoiding limited expansion of paste. Moulds were covered and samples were cured at 80° C for 24 h.

After demoulding cubical samples were prepared for investigation by cutting the specimens.

TABLE II
Mixture Composition of AAM

Mixture composition	Molar ratio		
	SiO_2/Al_2O_3	SiO_2/Na_2O	Na_2O/Al_2O_3
S0-0.30	0.77	4.58	0.17
S0-0.45	0.86	3.93	0.22
S0-0.60	0.94	3.52	0.27
S0-0.75	1.02	3.23	0.32
Al2S1-0.30	1.04	4.10	0.25
Al2S1-0.45	1.14	3.64	0.31
Al2S1-0.60	1.24	3.33	0.37
Al2S1-0.75	1.34	3.10	0.43
S1-0.30	1.55	5.08	0.30
S1-0.45	1.67	4.43	0.38
S1-0.60	1.79	3.98	0.45
S1-0.75	1.91	3.66	0.52

IV. Results and Discussion

A. Microstructure and Physical Properties

Highly porous AAM were obtained from all mixture designs. Microstructure of AAM material is given in Fig. 1. Large scale pores up to 4mm and specific surface in the range 4 to 6±1.0 g m^2/g ensures rapid water penetration inside the structure while small scale pores 0.1/0.5mm and capillary micropores <5µm could result in leaching over time.

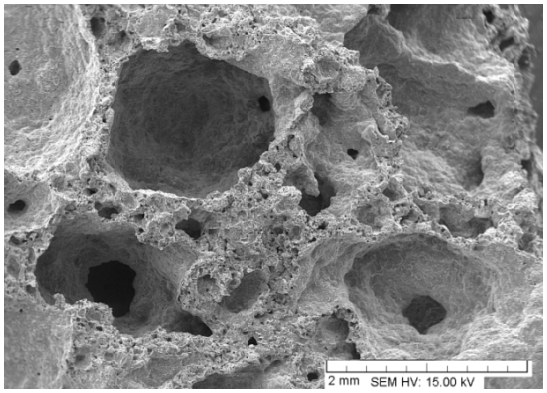

Fig. 1 Porous structure of AAM

Physical properties were measured and results are given in Table III. AAM density was in range from 346±17 to 484±15 kg/m^3 for mixtures with AAS-solid ratio >0.45. By increasing AAS-solid ratio material density decreased from9 to 21%due to increased NMR activity under high alkaline solution. Less porous AAM with increased density were obtained from the mixture designs with AAS-solid ratio 0.30; and the material density was in range from 675 to 797±20 kg/m^{3}due to the lower activity of NMR. This could be explained by decreasing alkalinity in AAM mixture during activation and material forming process which retarded gas emission from NMR.

Water absorption was affected by SiO_2/Na_2O ratio. Due to increased density of AAM samples with AAS-solid ratio 0.3, water absorption and porosity was lower comparing to the samples with AAS-solid ratio 0.45-0.75

For samples S0-0.30 water absorption was 45±2.3%, Al2S1-0.3 – 42±1.2%, S1-0.3 - 58±1.8%, respectively. Open and total porosity for samples with AAS-S ratio 0.3 was 31±1.1% and 73±0.5% for S0-0.3, 28±0.7% and 74±0.6% for Al2S1-0.3 and 29±1.1% and 80±1.7% for S1-0.3. By increasing AAS-solid ratio material porosity increased and reached 84±0.4 to 86±0.7% with ratio 0.75. By increasing AAS-solid ratio above 0.45, the porosity level has reached its maximum, consequently the physical properties being more similar among mixtures, which can be explained with reaching alkalinity limit, where the gas release from NMR was enhanced to maximum.

Water absorbtion of AAM increased with AAS-solid ratio increase for mixture S0 and Al2S0. By increasing AAS-solid ratio from 0.30 to 0.75, water absorbtion increased from 42±1.2 to 77±1.4%; however, open porosity decreased from 31±1.1 to 27±1.7% and total porosity increased from 73±0.5 to 86±2.1%. For mixture composition S1 water absorbtion and open porosity decrease was observed. This could be explained by the specific "glassy" phase of material with high SiO_2/Al_2O and Na_2O/Al_2O_3. The limit of total porosity for all mixtures was 84±0.4 to 86±0.8%.

B. pH Dynamics

After immersion of the prepared samples in deionized water batches, material capabilities to control pH over time were measured. The obtained pH curves are given in Fig. 2. Fig. 2 (a) represents pH changes over time for AAM contained NMR and MK(S0). The initial pH level in the first day of immersion increased from pH 10.5 (S0-0.30) to pH 11.79 (S0-0.75) together with the AAS-solid ratio increase from 0.30 to 0.75. Samples with AAS-solid ratio 0.45 to 0.75 provided almost linear pH decrease while in samples with lowest ratio S0-0.30 pH decrease was logarithmic with rapid initial decrease.

The final pH on deionized water in the batches where samples were immersed at 30thday was between 7.1 and 7.4. Similar tendency was observed for samples S1 and Al2S1. The initial pH after first day immersion in deionized water was in the range from pH 10.8 to 11.9and was slightly higher comparing to the mixture composition S0 (Fig. 2 (b) and (c)).

This could be explained by higher Na_2O content in mixture composition. The decrease of pH at the 30th day reached pH 7.1 for S1-0.3 and pH 8.1 to 8.4 for mixture with AAS-solid ratio 0.45-0.75. After 30 days decrease for Al2S1 to pH 6.8 for AAS-solid ratio 0.3 and pH 8.3 for 0.60 and 0.75 respectively was observed. For sample with ratio 0.45 pH decrease to 7.6 was observed (Fig. 2 (c)). The initial pH and final pH level could be contributed to the Na_2O ratio in the mixture composition. The higher content of Na_2O (Al2S1 and S1) was in the mixture, the higher initial and final pH was obtained. The decrease of final pH level indicates that alkalinity of all AAM has decreased and pH control limit has been reached.

Therefore pH curves could be divided in two groups. First group of pH curves could be described by the logarithmic curve which expresses the changes of pH for AAM with AAS-solid ratio 0.3. The average equation describing pH decrease could be expressed with equation

$$y = -1.0580 \pm 0.0461 \cdot \ln(x) + 10.8413 \pm 0.1380 \quad (7)$$

This low ratio provides reduced amount of free alkalis, therefore the initial pH was lower and decrease was noticeable at early test stage. pH decrease in the other group could be described with linear curve with average equation:

$$y = -0.1168 \pm 0.0123 \cdot x + 11.2120 \pm 0.2794 \quad (8)$$

The decrease of pH was gradual during 30 days. This trend was characteristic for mixture compositions with AAS-S ratio from 0.45 to 0.75.

TABLE III
PHYSICAL PROPERTIES AND LEACHING OF AAM

Property	Results											
	S0				S1				Al2S1			
AAS-solid ratio	**0.30**	**0.45**	**0.60**	**0.75**	**0.30**	**0.45**	**0.60**	**0.75**	**0.30**	**0.45**	**0.60**	**0.75**
Density	700	418	408	346	797	453	433	410	675	484	404	383
Water absorbtion, Wt%	45	67	67	77	58	58	52	51	42	58	66	69
Open porosity, %	31	28	28	27	29	26	23	21	28	27	27	27
Total porosity, %	73	84	84	86	80	82	83	84	74	81	84	85
Carbonate alkalinity,$CaCO_3$ eq ml/L/g	134	307	371	526	182	532	761	932	178	477	819	899
Bi-Carbonate alkalinity,$CaCO_3$ eq ml/L/g	298	311	315	270	329	219	210	200	276	227	237	218
Total alkalinity,$CaCO_3$eq ml/L/g	433	618	686	796	511	751	971	1132	454	704	1056	1117
Weight loss after leaching, 30 days, %	13.7	10.4	8.1	5.6	7.9	9.5	14.1	20.3	7.1	8.0	11.3	12.7

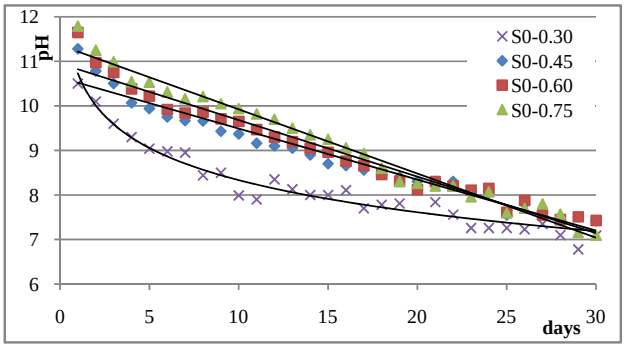

(a)

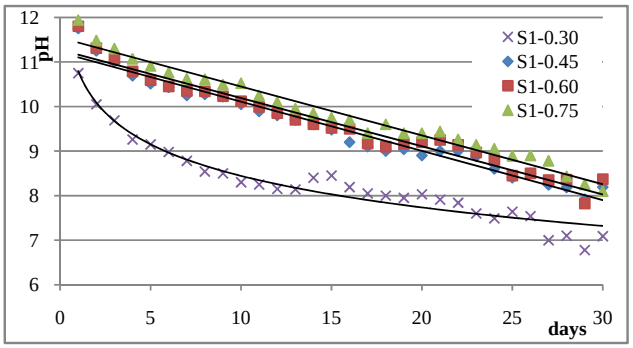

(b)

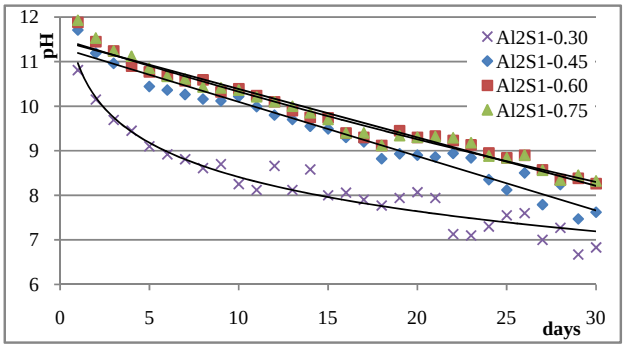

(c)

Fig. 2 pH dynamic curves during leaching test of AAM

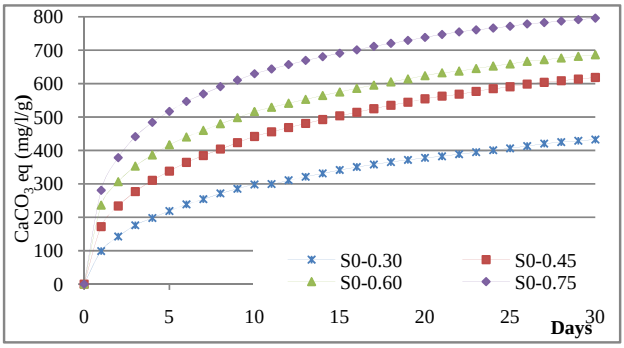

(a)

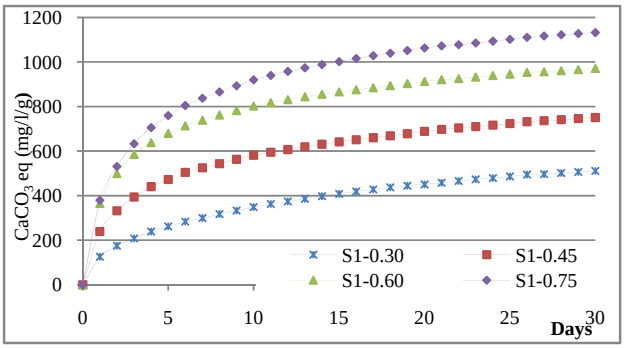

(b)

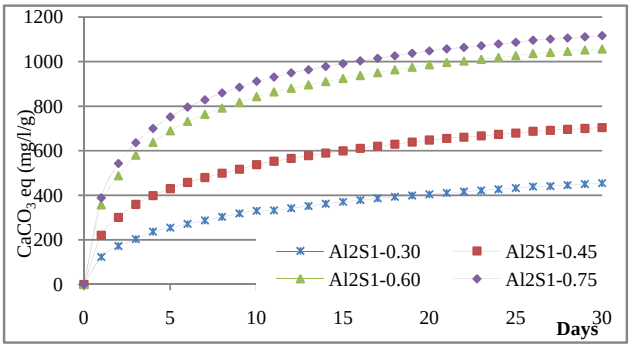

(c)

Fig. 3 Total alkalinity (TA) curves of AAM

C.AAM Buffer Capacity

The total alkalinity (TA) curves up to day 30 are given in Fig. 3. The TA curves provide continuous alkalinity increase during time and the amount of leached $CaCO_3$eq strongly depends from mixture composition and AAS-solid ratio. The TA curves increase in the first day was highest for all samples with AAS-solid ratio 0.75. For mixture composition S0 alkali leaching for the first day was 99, 172, 236 and 281 $CaCO_3$eq mg/l/g with regard to AAS-solid ratio from 0.30 to 0.75. The alkalis leached in the first day contained 23-35% from the total amount of leached alkalis. After the first day leaching of alkalis stabilizes for all S0 samples and the final TA reached 433, 618, 686, 796 $CaCO_3$eq mg/l/g at the age of 30 days (Fig. 3 (a)).

The maximum TA leaching was observed for the mixture composition S1 with the increased amount of Na_2O in composition. At the first day 125, 238, 365 and 379 mg/l/g $CaCO_3$eq was obtained or 25 to 38% from the total respectively. The final TA value was 511, 751, 971, 1132 mg/l/g $CaCO_3$ eq. TA curve for samples S1 is given in (Fig. 3 (b)). TA leaching increased from 118 to 142% comparing to S0.

The samples Al2S1 provided leaching of 123, 221, 356 and 388 mg/l/g $CaCO_3$eq during the first day (27 to 35% from total), which was very similar to mixture composition S1, and increase, comparing to S0, was 105 to 154%. For samples Al2S1 the final TA value at the 30th day was 454, 704, 1056 and 1116 mg/l/g $CaCO_3$eq (Fig. 3 (c)).

Comparing Al2S1 and S1, the difference of TA leaching was from 1-12% which leads to the conclusion that amount of NMR in mixture composition does not affect leaching of alkalis dramatically but the main factor impacting the leaching capacity is LSG and AAS-S ratio.

The results of CA are given in Fig. 4. The CA provides high initial pH value and high level of alkalinity of the solution.

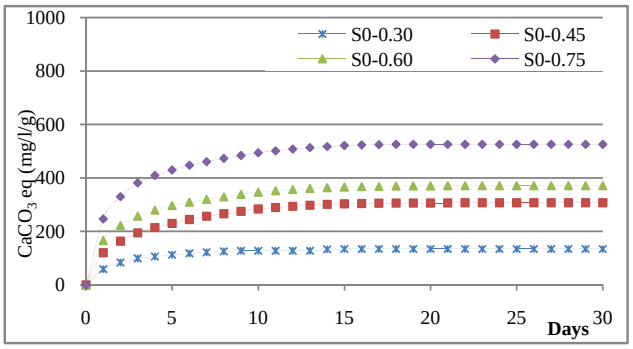

(a)

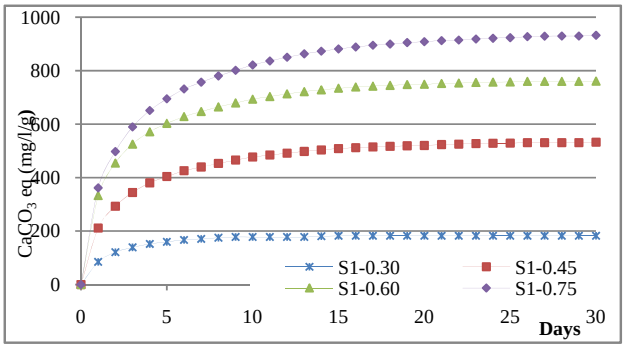

(b)

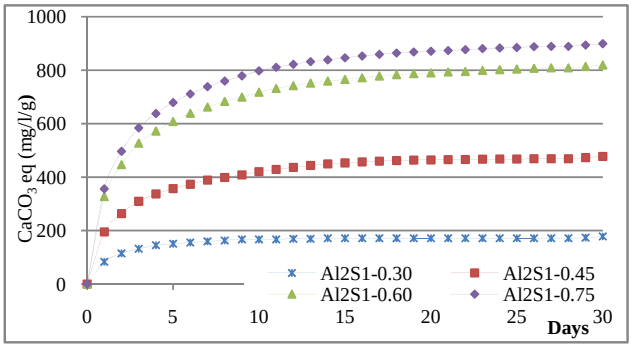

(c)

Fig. 4 Carbonate alkalinity (CA) curves of AAM

The CA leaching duration in the solution was affected by the Na_2O content in the mixture. The effective leaching of carbonate alkalis for mixture design S0 and with AAS-solid ratio lasted for 7 days reaching 122 from total 134 mg/l/g $CaCO_3$ eq. (91%). By increasing the AAS-solid ratio, duration of CA leaching could be increased up to 14 days when 517.5 from 526 mg/l/g $CaCO_3$ eq. (98%) was leached in solution for samples with AAS-solid ratio 0.75(Fig. 4a)).Mixture composition S1 provided the highest CA. Leaching of carbonate alkalis up to 21 days reached 912 from 932 mg/l/g $CaCO_3$ eq (98% leached). Dramatic decrease of CA leaching was observed for mixture with AAS-solid ratio 0.30 comparing with 0.75 respectively (Fig. 4 (b)).

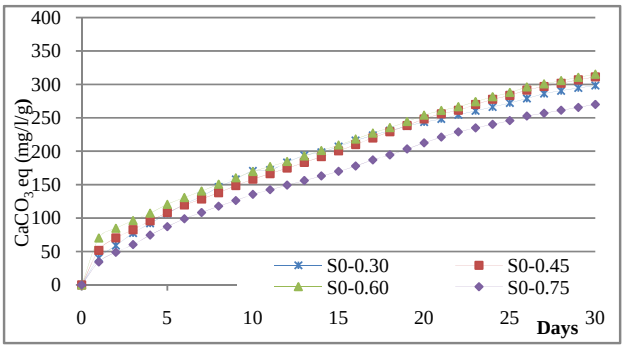

(a)

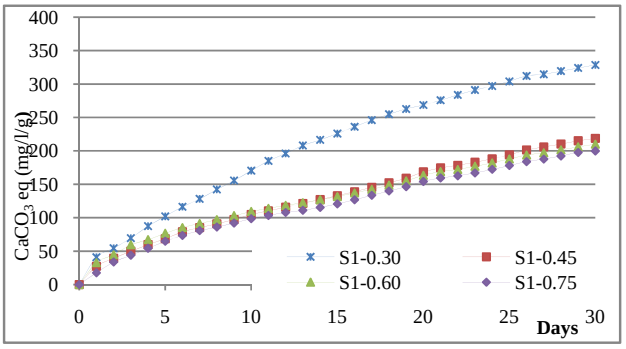

(b)

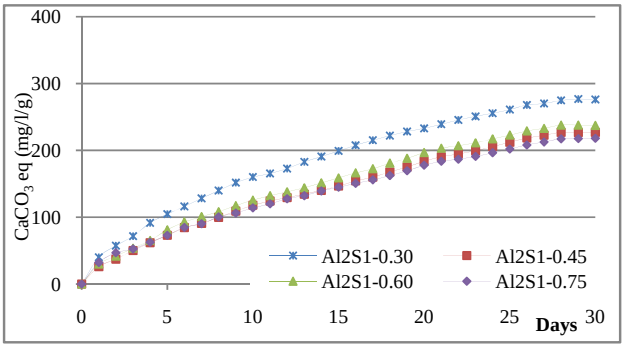

(c)

Fig. 5 Bi-carbonate alkalinity (BCA) curves of AAM

Al2S1 samples were with similar CA results as S1. CA could reach 899 mg/l/g $CaCO_3$eq at day 30 with AAS-solid ratio 0.75 while with 0.30 – 178 mg/l/g $CaCO_3$ eq respectively (Fig. 4 (c)).

The BCA contrary to the CA leached evenly in all testing period up to 30 days for all samples. The final BCA value

leached from samples is given in Fig. 5. The highest BCA was for samples S0. During testing period BCA was from 270-315 mg/l/g $CaCO_3$eq (Fig. 5 (a)). Samples S1 with AAS-solid ratio from 0.45 to 0.75 provided BCA from 200-219 mg/l/g $CaCO_3$ eq, while with 0.30 BCA was significantly higher - 329 mg/l/g $CaCO_3$eq respectively (Fig. 5 (b)).

The weight changes after alkalinity test was measured. It was detected that mass decreased for all specimens (Table III). For mixture design S0 weight loss was from 5.6-13.7%. The highest loss was for samples with AAS-solid ratio 0.3. For samples S1 weight loss was from 7.9 to 20.3% and for Al2S1 from 7.1 to 12.7%. Samples with higher AAS-solid ratio lost more weight– 0.75. This could be explained by relatively high amount of leaching alkalis.

V. Conclusion

The leaching of alkalis in water was mainly affected by the AAS-S ratio and LSG additive in mixture composition with high SiO_2/Al_2O_3 and Na_2O/Al_2O_3.A physical property of AAM, such as open porosity, was a secondary aspect of leaching effect. High SiO_2 and Na_2O content ensures maximal leaching of alkalis in solution, while increased quantity of Al_2O_3limits alkali leaching. This could be contributed to the AAM structure formation, where Al_2O_3 is one of the key factors of creating AAM.

By changing the mixture composition, material with different pH values and alkalinity could be created, which would be useful in biogas reactors, where pH level must be controlled during the anaerobic digestion process. By choosing proper mixture proportions and amount of AAM, the necessary pH value could be obtained to achieve the most efficient biomethane potential.

Acknowledgment

This work has been supported by ESF project „Involvement of Human Resources for Development of Integrated Renewable Energy Resources Energy Production System", No. Nr.2013/0014/1DP/1.1.1.2.0/13/APIA/VIAA/026.

References

[1] F. Malaspina, C. M. Cellamare, L. Stante, and A. Tilche, "Anaerobic treatment of cheese whey with a downflow-upflow hybrid reactor," Bioresour. Technol., vol. 55, pp. 131–139, 1996.

[2] S. Montalvo, L. Guerrero, R. Borja, E. Sánchez, Z. Milán, I. Cortés, and M. Angeles de la laRubia, "Application of natural zeolites in anaerobic digestion processes: A review," Applied Clay Science, vol. 58. pp. 125–133, 2012.H. Poor, *An Introduction to Signal Detection and Estimation*. New York: Springer-Verlag, 1985, ch. 4.

[3] A. Saddoud, I. Hassaïri, and S. Sayadi, "Anaerobic membrane reactor with phase separation for the treatment of cheese whey," Bioresour. Technol., vol. 98, pp. 2102–2108, 2007.E. H. Miller, "A note on reflector arrays (Periodical style—Accepted for publication)," *IEEE Trans. Antennas Propagat.*, to be published.

[4] K. Rugele, G. Bumanis, L. Erina, and D. Erdmane, "Composite Material for Effective Cheese Whey Anaerobic Digestion," Key Eng. Mater., vol. 604, pp. 236–239, Mar. 2014.C. J. Kaufman, Rocky Mountain Research Lab., Boulder, CO, private communication, May 1995.

[5] M. C. G. Juenger, F. Winnefeld, J. L. Provis, and J. H. Ideker, "Advances in alternative cementitious binders," Cem. Concr. Res., vol. 41, no. 12, pp. 1232–1243, Dec. 2011.M. Young, *TheTechincal Writers Handbook.* Mill Valley, CA: University Science, 1989.

[6] C. Li, H. Sun, and L. Li, "A review: The comparison between alkali-activated slag (Si+Ca) and metakaolin (Si+Al) cements," Cem. Concr. Res., vol. 40, no. 9, pp. 1341–1349, Sep. 2010.

[7] S. A. Bernal, R. Mejía de Gutiérrez, and J. L. Provis, "Engineering and durability properties of concretes based on alkali-activated granulated blast furnace slag/metakaolin blends," Constr. Build. Mater., vol. 33, pp. 99–108, Aug. 2012.

[8] A. Fernández-Jiménez, M. Monzó, M. Vicent, a. Barba, and a. Palomo, "Alkaline activation of metakaolin–fly ash mixtures: Obtain of Zeoceramics and Zeocements," MicroporousMesoporous Mater., vol. 108, no. 1–3, pp. 41–49, Feb. 2008.

[9] C. E. White, J. L. Provis, A. Llobet, T. Proffen, and J. S. J. van Deventer, "Evolution of Local Structure in Geopolymer Gels: An In Situ Neutron Pair Distribution Function Analysis," J. Am. Ceram. Soc., vol. 94, no. 10, pp. 3532–3539, Oct. 2011.

[10] S. Alonso and A. Palomo, "Alkaline activation of metakaolin and calcium hydroxide mixtures: influence of temperature, activator concentration and solids ratio," Mater. Lett., no. Jan. 2001.

[11] J. Temuujin, A. Minjigmaa, W. Rickard, M. Lee, I. Williams, and A. van Riessen, "Preparation of metakaolin based geopolymer coatings on metal substrates as thermal barriers," Appl. Clay Sci., vol. 46, no. 3, pp. 265–270, Nov. 2009.

[12] J. Temuujin, a van Riessen, and R. Williams, "Influence of calcium compounds on the mechanical properties of fly ash geopolymerpastes.," J. Hazard. Mater., vol. 167, no. 1–3, pp. 82–8, Aug. 2009.

[13] M. R. Rowles and B. H. O'Connor, "Chemical and Structural Microanalysis of AluminosilicateGeopolymers Synthesized by Sodium Silicate Activation of Metakaolinite," J. Am. Ceram. Soc., vol. 92, no. 10, pp. 2354–2361, Oct. 2009.

[14] S. a. Bernal, R. M. de Gutierrez, J. L. Provis, and V. Rose, "Effect of silicate modulus and metakaolin incorporation on the carbonation of alkali silicate-activated slags," Cem. Concr. Res., vol. 40, no. 6, pp. 898–907, June. 2010.

[15] C. K. Yip, G. C. Lukey, J. L. Provis, and J. S. J. van Deventer, "Effect of calcium silicate sources on geopolymerisation," Cem. Concr. Res., vol. 38, no. 4, pp. 554–564, Apr. 2008.

[16] P. Duxson, J. L. Provis, G. C. Lukey, and J. S. J. van Deventer, "The role of inorganic polymer technology in the development of 'green concrete,'" Cem. Concr. Res., vol. 37, no. 12, pp. 1590–1597, Dec. 2007.

[17] C. K. Yip, G. C. Lukey, and J. S. J. van Deventer, "The coexistence of geopolymeric gel and calcium silicate hydrate at the early stage of alkaline activation," Cem. Concr. Res., vol. 35, no. 9, pp. 1688–1697, Sep. 2005.

[18] G. Bumanis, D. Bajare, and J. Locs, "The Effect of Activator on the Properties of Low-Calcium Alkali-Activated Mortars," Key Eng. Mater., vol. 604, pp. 169–172, Mar. 2014.

[19] W. K. W. Lee and J. S. J. van Deventer, "The effect of ionic contaminants on the early-age properties of alkali-activated fly ash-based cements," Cem. Concr. Res., vol. 32, no. 4, pp. 577–584, Apr. 2002.

[20] P. Duxson, G. C. Lukey, F. Separovic, and J. S. J. van Deventer, "Effect of Alkali Cations on Aluminum Incorporation in Geopolymeric Gels," Ind. Eng. Chem. Res., vol. 44, no. 4, pp. 832–839, Feb. 2005.

[21] S. Hong and F. P. Glasser, "Alkali sorption by C-S-H and C-A-S-H gels Part II . Role of alumina," Cem. Concr. Res., vol. 32, no. 7, pp. 1101–1111, 2002.

[22] R. R. Lloyd, J. L. Provis, and J. S. J. van Deventer, "Pore solution composition and alkali diffusion in inorganic polymer cement," Cem. Concr. Res., vol. 40, no. 9, pp. 1386–1392, Sep. 2010.

[23] D. Bajare, A. Korjakins, J. Kazjonovs, and I. Rozenstrauha, "Pore structure of lightweight clay aggregate incorporate with non-metallic products coming from aluminium scrap recycling industry," J. Eur. Ceram. Soc., vol. 32, pp. 141–148, 2012.

[24] D. Bajare, A. Korjakins, and J. Kazjonovs, "Application of Aluminium Dross and Glass Waste for Production of Expanded Clay Aggregate," in Civil Engineering '11 - 3rd International Scientific Conference, Proceedings, 2011, vol. 3, pp. 27–31.

[25] Snoeyink, V.L. and D. Jenkins, Water Chemistry. New York: John Wiley & Sons, 1980.